Cooling with fermionic thermal reservoirs

Gabriella G. Damas,[1] Rogério J. de Assis,[1,2] and Norton G. de Almeida[1]
[1]*Instituto de Física, Universidade Federal de Goiás, 74.001-970 Goiânia-GO, Brazil*
[2]*Departamento de Física, Universidade Federal de São Carlos, 13.565-905 São Carlos-São Paulo, Brazil*

(Received 18 July 2022; accepted 6 March 2023; published 17 March 2023)

The quantum reservoirs commonly considered in open-quantum systems theory are those modeled by quantum harmonic oscillators, which are called bosonic reservoirs. Recently, quantum reservoirs modeled by two-level systems, the so-called fermionic reservoirs, have received attention due to their features. Given that the components of these reservoirs have a finite number of energy levels, unlike bosonic reservoirs, some studies are being carried out to explore the advantages of using this type of reservoir, especially in the operation of heat machines. In this paper, we carry out a case study of a quantum refrigerator operating in the presence of bosonic or fermionic thermal reservoirs, and we show that fermionic baths have advantages over bosonic ones.

DOI: 10.1103/PhysRevE.107.034128

I. INTRODUCTION

With the development of the so-called quantum thermodynamics [1–3], there is an increasing interest in the realization of thermal devices operating at the quantum limit [4–10]. In particular, heat engines whose working substance consists of systems with quantized energy levels, such as two-level systems (qubits) and quantum harmonic oscillators, can absorb from or deliver to their surroundings quantities of energy as small as their corresponding energy gaps. Comparative studies exploring the difference between working substances with finite and infinite energy levels demonstrate that heat engines operating with the first kind of working substance can present advantages [11–14]. Particularly, systems with finite energy levels, such as qubits, can exhibit stationary states with population inversion [15–17], giving rise to negative temperatures [18,19]. This inverted population effect has been explored in some works [20–22] with a remarkable impact on the efficiency of heat engines, as experimentally shown in Refs. [17,22]. The population inversion associated with the negative temperature of the working substance requires a reservoir whose average number of photons n_F with energy E is given by the Fermi-Dirac distribution $n_F = 1/(e^{E/T} + 1)$, where T is the temperature of the reservoir. Since $0 < n_F < 1$, it is straightforward to see that $0 < n_F < 1/2$ $(1/2 < n_F < 1)$ implies $T > 0$ $(T < 0)$. This sort of reservoir requires components with a limited spectrum and for this reason are commonly modeled by two-level systems, thus, being called fermionic reservoirs [11,15,16,22–29]. Although the temperatures of fermionic reservoirs assume both positive and negative values, reservoirs with $T > 0$ are mostly modeled by quantum harmonic oscillators with the average number of photons given by the Bose-Einstein distribution $n_B = 1/(e^{E/T} - 1)$, which makes them known as bosonic reservoirs. Note that bosonic reservoirs cannot reach negative temperatures since $0 < n_B < \infty$.

Heat engines operating in the quantum regime are typically called quantum heat engines. Another kind of quantum device widely discussed in quantum thermodynamics is the so-called quantum refrigerator [30–33]. In this paper, we consider a case study in which a quantum refrigerator built with qubits can present advantages when operating in a fermionic environment compared to a bosonic one. We assume all reservoirs with positive temperatures (thermal reservoirs). As the operating conditions are kept the same for both environments, our results emphasize that the presented advantage stems from the quantum nature of the fermionic thermal reservoir.

II. MODEL

In the present paper, we consider a self-contained quantum refrigerator (SCQR) composed of three interacting qubits, each in contact with a specific thermal reservoir. The respective SCQR was first proposed in Ref. [25] in which the authors took into account only bosonic thermal reservoirs. Although the authors have also addressed qutrits and systems with more energy levels, which may be interesting for engineering quantum refrigerators, for a better comparison of the effect of different types of thermal reservoirs on the cooling percentages, we will restrict our study to the SCQR composed of three qubits. Recently, we investigated this SCQR operating with one of the reservoirs being a fermionic one at a negative temperature, see Ref. [34]. Here, as in Ref. [25], we approach the case in which qubits 1–3 interact, respectively, with a thermal reservoir at a cold temperature $T_c > 0$, a thermal reservoir at a room-temperature $T_r > 0$, and a thermal reservoir at a hot temperature $T_h > 0$—see the schematic shown in Fig. 1. The device in question works, such as a refrigerator when $T_1 - T_c < 0$, where T_1 is the temperature of qubit 1. In this case, therefore, heat flows from the cold thermal reservoir to qubit 1. However, considering the asymptotic state, this only occurs if the relations $E_3 = E_2 - E_1$ with $E_k > 0$ being the energy gap of qubit k $(k = 1–3)$, and $T_c < T_r < T_h$ are satisfied [25].

We assume the weak-coupling limit and the Markovian regime governing the dynamics of the SCQR such that the

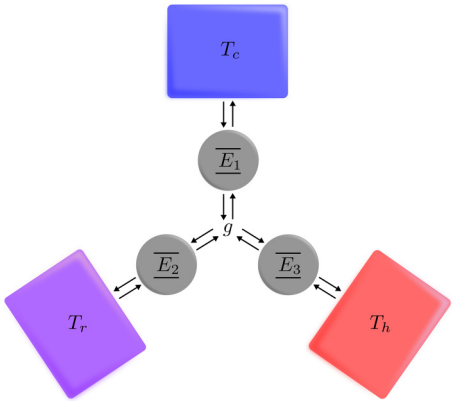

FIG. 1. Schematic of the SCQR refrigerator and its respective thermal reservoirs. The SCQR is composed of three interacting qubits having energy gaps E_1–E_3 in contact with their respective thermal reservoirs. Here, T_h is the temperature of the hot thermal reservoir, T_r is the temperature of the "room" thermal reservoir, T_c is the temperature of the cold thermal reservoir, and g is the coupling constant between the qubits.

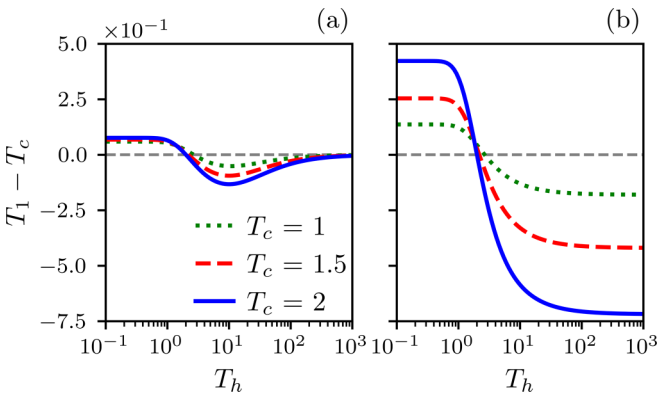

FIG. 2. Temperature difference $T_1 - T_c$ versus T_h for (a) three bosonic and (b) three fermionic thermal reservoirs, considering three different values of T_c: $T_c = 1$ (dotted green line), $T_c = 1.5$ (dashed red line), and $T_c = 2$ (solid blue line). Refrigeration occurs for $T_1 - T_c < 0$. Note the difference in behavior in the two figures: whereas, in (a) temperature T_1 reaches a minimum and then starts to increase, approaching zero, in (b) T_1 decreases monotonically, practically stabilizing for sufficiently high T_h, thus, indicating that the lowest temperatures reached by qubit 1 occur for fermionic thermal reservoirs.

master equation is [26,35]

$$\frac{d\rho}{dt} = -i[H_0 + H_{\rm int}, \rho] + \sum_{k=1}^{3} \frac{\Gamma^{\downarrow}_{B(F),k}}{2}(2\sigma_{-,k}\rho\sigma_{+,k} - \{\sigma_{+,k}\sigma_{-,k}, \rho\}) + \sum_{k=1}^{3} \frac{\Gamma^{\uparrow}_{B(F),k}}{2}(2\sigma_{+,k}\rho\sigma_{-,k} - \{\sigma_{-,k}\sigma_{+,k}, \rho\}). \quad (1)$$

Here, the free qubits Hamiltonian H_0 and the three-body interaction Hamiltonian $H_{\rm int}$ are given by

$$H_0 = \frac{E_1}{2}\sigma_{z,1} + \frac{E_3}{2}\sigma_{z,3} + \frac{E_3}{2}\sigma_{z,3}, \quad (2)$$

and

$$H_{\rm int} = g(\sigma_{-,1}\sigma_{+,2}\sigma_{-,3} + \sigma_{+,1}\sigma_{-,2}\sigma_{+,3}), \quad (3)$$

where $\sigma_{z,k}$ is the z Pauli operator for qubit k, g is the coupling constant, and $\sigma_{-,k}$ ($\sigma_{+,k}$) is the lowering (raising) Pauli operator for qubit k. Note that Eq. (1) governs the dynamics of either bosonic [35] and fermionic [23,24,26,36] thermal reservoirs: if qubit k is interacting with a bosonic (fermionic) thermal reservoir, $\Gamma^{\downarrow}_{B,k} = \gamma_k(1 + n_{B,k})$ ($\Gamma^{\downarrow}_{F,k} = \gamma_k(1 - n_{F,k})$) and $\Gamma^{\uparrow}_{B,k} = \gamma_k n_{B,k}$ ($\Gamma^{\uparrow}_{F,k} = \gamma_k n_{F,k}$), where γ_k is the dissipation rate and $n_{B,k} = 1/(e^{E_k/T_{\phi_k}} - 1)$ ($n_{F,k} = 1/(e^{E_k/T_{\phi_k}} + 1)$) is the average excitation number, being $\phi_1 = c$, $\phi_2 = r$, and $\phi_3 = h$. See that since $n_{F,k} < 1/2$ for $T_{\phi_k} > 0$, then $\Gamma^{\downarrow}_{B,k}$ ($\Gamma^{\uparrow}_{B,k}$) is always greater than $\Gamma^{\downarrow}_{F,k}$ ($\Gamma^{\uparrow}_{F,k}$). To obtain the asymptotic state of Eq. (1) we used the quantum optics toolbox [37,38].

III. RESULTS

Since the exchange rates $\Gamma^{\downarrow}_{B,k}$ ($\Gamma^{\uparrow}_{B,k}$) and $\Gamma^{\downarrow}_{F,k}$ ($\Gamma^{\uparrow}_{F,k}$) are different, the possible combinations of bosonic and fermionic thermal reservoirs lead to distinct asymptotic states of Eq. (1). So, aiming to use the device as a refrigerator, it is interesting to evaluate which combination leads to the lowest-temperature T_1, considering a given set of parameters. To compare the SCQR operating in the different configurations, we start by fixing the energies $E_1 = 1$, $E_2 = 5$, and $E_3 = 4$; the temperatures $T_c = 1$, 1.5, 2, and $T_r = 2$; the coupling constant $g = 10^{-2}$; and the dissipation rates $\gamma_1 = \gamma_2 = \gamma_3 = g$. Next, we let T_h vary from 10^{-1} to 10^3.

Figure 2(a) shows the temperature difference $T_1 - T_c$ versus T_h (on logarithmic scale) for the SCQR working in a bosonic environment for the cold temperatures $T_c = 1$ (dotted green line), $T_c = 1.5$ (dashed red line), and $T_c = 2$ (solid blue line). As said before, cooling occurs when $T_1 - T_c < 0$. Similarly, Fig. 2(b) shows $T_1 - T_c$ as a function of T_h for the same cold temperatures, but now the SCQR is surrounded by fermionic thermal reservoirs. In Fig. 2(a), $T_1 - T_c$ decreases to a minimum value and then increases until it stabilizes at a negative value close to zero, whereas, in Fig. 2(b), $T_1 - T_c$ stabilizes at its minimum value. Thus, the SCQR in the fermionic environment has an advantage over the bosonic one, as its efficiency in cooling qubit 1 does not decrease at higher values of T_h. Furthermore, under fermionic thermal reservoirs, qubit 1 reaches lower minimum temperature values than when under bosonic thermal reservoirs, as can be seen from the difference $T_1 - T_c$, which is more negative for the fermionic environment (compare Figs. 2(a) and 2(b)).

According to our numerical simulations, when considering the bosonic environment, the minimum values for T_1 are $T_1 \sim 0.95$ (when $T_c = 1$), $T_1 \sim 1.41$ (when $T_c = 1.5$), and $T_1 \sim 1.87$ (when $T_c = 2$). On the other hand, when considering three fermionic thermal reservoirs since the values for T_1 continue to decrease with increasing T_h, we take the minimum value for T_1 when $T_h = 100$. These minimum values are $T_1 \sim 0.82$ (when $T_c = 1$), $T_1 \sim 1.09$ (when $T_c = 1.5$), and $T_1 \sim 1.29$ (when $T_c = 2$). By considering T_c as a reference, we can then calculate the cooling percentage $(|T_1 - T_c|/T_c) \times$

TABLE I. Comparative values in the cooling percentage $(|T_1 - T_c|/T_c) \times 100$ for the refrigerator working at three bosonic (3B) and three fermionic (3F) thermal reservoirs for three values of the reference temperature T_c.

	(%)	
T_c	3B	3F
1	5.14	17.57
1.5	6.31	27.44
2	6.65	35.32

100 to compare how much the fermionic and bosonic thermal reservoirs cools qubit 1 - see Table I, where 3B (3F) stands for three bosonic (fermionic) reservoirs.

Table I shows a significant difference in the cooling percentage for the two sets of thermal reservoirs: it is always higher when using three fermionic thermal reservoirs, thus, clearly showing that the fermionic environment is far more efficient in decreasing the temperature T_1 than the bosonic one. Also, this percentage is better the higher the reference temperature T_c such that for $T_c = 2$, it can reach up to more than four times the value reached using only bosonic thermal reservoirs. For lower values of the cold temperatures T_c, the percentage difference decreases, but using fermionic thermal reservoirs, the cooling when $T_c = 1$ is still more than double that of the case of bosonic thermal reservoirs alone. It is worth mentioning that by fixing the SCQR parameters as we did, there is a limit to cooling qubit 1. As we found numerically, the corresponding lowest cooling percentage reached by qubit 1, irrespective of the type of thermal reservoir used, occurs when $T_c \sim 0.48$. For temperatures lower than $T_c \sim 0.48$, $T_1 - T_c > 0$, meaning that the SCQR no longer works. Also, the percentage of cooling decreases more and more as T_c approaches 0.48 for both kinds of thermal reservoirs. However, the percentage of cooling when using fermionic thermal reservoirs remains higher as shown in Table II.

As we have seen, for fixed parameters we cannot cool down qubit 1 to zero absolute. However, there is a strategy to keep up cooling toward zero absolute, which is to isolate qubit 1 from its environment. This condition, obtained by imposing $\gamma_1 \to 0$ or equivalently $\Gamma^{\downarrow}_{B(F),1} \to 0$ and $\Gamma^{\uparrow}_{B(F),1} \to 0$ in (1), allows us to obtain the following analytical solution for the

TABLE II. Comparative values show that the cooling percentages $(|T_1 - T_c|/T_c) \times 100$ for fixed parameters decrease as the reference temperature T_c approaches 0.48, where $T_1 - T_c > 0$. Note that even so fermionic thermal reservoirs are always more effective for cooling.

	(%)	
T_c	3B	3F
0.48	0.87	3.31
0.60	2.20	7.39
0.80	4.14	12.85

TABLE III. Comparative values showing the cooling percentages $(|T_1 - T_c|/T_c) \times 100$ for several thermal reservoir configurations. Here, for example, BFF means qubit 1 bound to a bosonic thermal reservoir and qubits 2 and 3 bound to fermionic thermal reservoirs. Note that the highest percentage of cooling occurs for the FBF configuration, meaning that qubit 1 is bound to a fermionic thermal reservoir, qubit 2 is bound to a bosonic thermal reservoir and qubit 3 is bound to another fermionic thermal reservoir.

	(%)							
T_c	FBF	FFF	FBB	FFB	BBF	BFF	BBB	BFB
0.48	3.38	3.31	1.11	1.10	2.71	2.65	0.87	0.86
0.80	13.09	12.85	7.31	7.22	7.76	7.62	4.14	4.09
1	17.87	17.57	10.81	10.67	9.03	8.87	5.14	5.09
1.5	27.28	27.44	18.65	18.43	10.28	10.13	6.31	6.24
2	35.76	35.32	25.36	25.09	10.46	10.33	6.65	6.58

temperature of qubit 1,

$$T_1 = \frac{T_c}{1 + \frac{E_3}{E_1}\left(1 - \frac{T_c}{T_h}\right)}, \tag{4}$$

from which we can see that, if we let $E_3/E_1 \to \infty$, then $T_1 \to 0$. This result, obtained in Ref. [25], shows that there is no fundamental limit to cool down to zero absolute, provided we can perfectly isolate qubit 1.

So far we have considered fermionic thermal reservoirs for all qubits in the SCQR. Other possibilities include the cases of combinations of bosonic and fermionic thermal reservoirs. In fact, considering the fermionic thermal reservoir as a quantum resource, it may be interesting to consider cases where only one or two fermionic thermal reservoirs are used. For this, it is necessary to consider which qubit the fermionic thermal reservoir is associated with. Let us use a notation in which B (F) denotes the bosonic (fermionic) thermal reservoir and the order in which it appears in the sequence indicates which qubit that reservoir is attached to. For example, the sequence BFB indicates that qubit 1 is subjected to a bosonic thermal reservoir, qubit 2 to a fermionic thermal reservoir, and the third qubit to a bosonic thermal reservoir. Next, we investigate all configurations numerically and grouped the results in Table III, ordering from highest to lowest percentage of cooling and following the same procedure as in the previous tables, i.e., we took the minimum value for T_1.

Interestingly, and contrary to what one might think, the best case does not occur when three fermionic thermal reservoirs are used. As Table III shows, the greatest cooling range occurs for the FBF case, i.e., when only qubits 1 and 3 are bound to fermionic thermal reservoirs. Although the difference between the FBF and FFF configurations is small, it is still notable that the cooling percentage is higher when only two fermionic reservoirs are used instead of three. As mentioned at the beginning of this section, this difference is due to the discrepancy between the exchange rates $\Gamma^{\downarrow}_{B,k}$ ($\Gamma^{\uparrow}_{B,k}$) and $\Gamma^{\downarrow}_{F,k}$ ($\Gamma^{\uparrow}_{F,k}$) since they determine the asymptotic state of Eq. (1).

IV. CONCLUSION

Recent studies on quantum heat machines have used quantum reservoirs as a resource to obtain better performances both in engines and refrigerators [12,20,21,39]. For example, fermionic reservoirs have been explored in previous works, especially in their purely quantum characteristic of presenting population inversion [17,22], which, in turn, is associated with negative temperatures [3,18]. Here, we explore the quantum nature of fermionic reservoirs without taking population inversion into account such that we restrict to the domain of positive temperatures. Using a qubit-based refrigerator model proposed in Ref. [25], we show that, once the operating parameters of the refrigerator are fixed, the use of fermionic thermal reservoirs allows us to obtain better results, concerning the cooling capacity, than the use of bosonic thermal reservoirs. We have verified, for example, that when the qubit to be cooled cannot be perfectly insulated, the use of only fermionic thermal reservoirs allows it to reach lower temperatures than the use of only bosonic thermal reservoirs. In addition, contrary to what might be thought, the cooling can be more effective, in the sense of obtaining a higher percentage of cooling, when instead of three, only two fermionic thermal reservoirs are used. As a final remark, we would like to emphasize that our results are limited to the quantum refrigerator studied here. We hope that our findings will motivate the quantum thermodynamics community to continue investigating to better understand the origin of the cooling advantages stemming from combining fermionic and bosonic reservoirs.

ACKNOWLEDGMENTS

We acknowledge financial support from the Brazilian agencies: Coordenação de Aperfeiçoamento de Pessoal de Nível Superior (CAPES), Financial Code No. 001; National Council for Scientific and Technological Development (CNPq), Grants No. 311612/2021-0 and No. 301500/2018-5; São Paulo Research Foundation (FAPESP), Grant No. 2021/04672-0; Goiás State Research Support Foundation (FAPEG). This work was performed as part of the Brazilian National Institute of Science and Technology (INCT) for Quantum Information, Grant No. 465469/2014-0.

APPENDIX: DERIVING THE MASTER EQUATION

Let us start the derivation of the master equation assuming we have a two-level system S that is coupled to a fermionic reservoir R. In this case, the Hamiltonian corresponding to our two-level system is

$$H_S = \hbar\omega_0\sigma_+\sigma_-, \tag{A1}$$

where ω_0 refers to the frequency, σ_+ and σ_- are, respectively, the creation and annihilation operator for the two-level system. The fermionic reservoir is composed by a collection of noninteracting two-level systems whose Hamiltonian is

$$H_R = \hbar\sum_j \omega_j\sigma_{+,j}\sigma_{-,j}, \tag{A2}$$

here ω_j represents the jth frequency of the reservoir. Furthermore, the Hamiltonian of interaction between the system and the reservoir has the form

$$H_{\rm SR} = \hbar\sum_j(\kappa_j^*\sigma_-\sigma_{+,j} + \kappa_j\sigma_+\sigma_{-,j}), \tag{A3}$$

with κ_j being the jth coupling constant.

The dynamics of the composite system $S\otimes R$ is given by the Von Neumann equation,

$$\dot\chi(t) = \frac{1}{i\hbar}[V,\chi(t)], \tag{A4}$$

where χ and V are, respectively, the density operator and the Hamiltonian of the composite system in the interaction picture. Integrating Eq. (A4), and substituting the result back into Eq. (A4), gives

$$\dot\chi(t) = \frac{1}{i\hbar}[V(t),\chi(t)] - \frac{1}{\hbar^2}\int_0^t dt'\{V(t),[V(t'),\chi(t')]\}, \tag{A5}$$

with $\chi(0)=\rho(0)\otimes R_0$, being $\rho(0)$ and R_0 the initial states of S and R, respectively. The initial state of the reservoir is the Gibbs state,

$$R_0 = \frac{e^{-\beta H_R}}{{\rm tr}_R(e^{-\beta H_R})}, \tag{A6}$$

which can also be written as

$$R_0 = \prod_j \frac{e^{(-\beta\hbar/2)\omega_j\sigma_{z,j}}}{e^{(-\beta\hbar/2)\omega_j}+e^{(-\beta\hbar/2)\omega_j}}. \tag{A7}$$

Now, the dynamics of the system of interest S is obtained by tracing over the reservoir variables in Eq. (A5), which provides

$$\dot\rho(t) = \frac{1}{i\hbar}\{{\rm tr}_R[V(t)R_0]\rho(0) - \rho(0){\rm tr}_R[R_0V(t)]\} - \frac{1}{\hbar^2}\int_0^t dt'{\rm tr}_R(\{V(t),[V(t'),\chi(t')]\}). \tag{A8}$$

Considering that ${\rm tr}_R[V(t)R_0]=0$, what is satisfied by R_0 of the Eq. (A6), Eq. (A8) becomes

$$\dot\rho(t) = -\frac{1}{\hbar^2}\int_0^t dt'{\rm tr}_R(\{V(t),[V(t'),\chi(t')]\}). \tag{A9}$$

Assuming the Born approximation $\chi(t)\approx\rho(t')\otimes R_0$, see Refs. [35,36], we arrive at

$$\dot\rho(t) = -\frac{1}{\hbar^2}\int_0^t dt'{\rm tr}_R(\{V(t),[V(t'),\rho(t')\otimes R_0]\}). \tag{A10}$$

By writing Eq. (A3) in the interaction picture, noting that ${\rm tr}_R(\sigma_{\pm,j}\sigma_{\pm,k}R_0)=0$, Eq. (A10) becomes

$$\begin{aligned}\dot\rho(t) = -\int_0^t dt'\{&[\sigma_-\sigma_+\rho(t') - \sigma_+\rho(t')\sigma_-]\\ &\times e^{-i\omega_0(t-t')}\langle F^\dagger(t)F(t')\rangle_R\\ &+[\rho(t')\sigma_+\sigma_- - \sigma_-\rho(t')\sigma_+]\\ &\times e^{-i\omega_{0,k}(t-t')}\langle F(t')F^\dagger(t)\rangle_R + {\rm H.c.}\},\end{aligned} \tag{A11}$$

where the reservoir averages read

$$\langle F^{\dagger}(t)F(t')\rangle_R = \sum_j |\kappa_j|^2 e^{i\omega_j(t-t')}\bar{n}(\omega_j,\beta) \tag{A12}$$

and

$$\langle F(t')F^{\dagger}(t)\rangle_R = \sum_j |\kappa_j|^2 e^{i\omega_j(t-t')}[1-\bar{n}(\omega_j,\beta)]. \tag{A13}$$

with $\bar{n}(\omega,\beta)$ being the average number of excitation of the fermionic bath given by the Fermi-Dirac distribution,

$$\bar{n}(\omega_j,\beta) = \frac{1}{e^{\hbar\beta\omega_j}+1}. \tag{A14}$$

Carrying out the changes $\tau = t-t'$ and $\sum_j \to \int_0^\infty d\omega\, g(\omega)$, results in

$$\begin{aligned}\dot{\rho}(t) = -\int_0^t d\tau \{&[\sigma_-\sigma_+\rho(t-\tau) - \sigma_+\rho(t-\tau)\sigma_-]\\ &\times e^{-i\omega_0\tau}\langle F^{\dagger}(t)F(t-\tau)\rangle_R\\ &+[\rho(t-\tau)\sigma_+\sigma_- - \sigma_-\rho(t-\tau)\sigma_+]\\ &\times e^{-i\omega_0\tau}\langle F(t-\tau)F^{\dagger}(t)\rangle_R + \text{H.c.}\},\end{aligned} \tag{A15}$$

with

$$\langle F^{\dagger}(t)F(t-\tau)\rangle_R = \int_0^\infty d\omega\, g(\omega)|\kappa(\omega)|^2 e^{i\omega\tau}\bar{n}(\omega,\beta), \tag{A16}$$

and

$$\langle F(t-\tau)F^{\dagger}(t)\rangle_R = \int_0^\infty d\omega\, g(\omega)|\kappa(\omega)|^2 e^{i\omega\tau}[1-\bar{n}(\omega,\beta)]. \tag{A17}$$

Performing the Markov approximation, which consists of replacing $\rho(t-\tau)$ with $\rho(t)$ in Eq. (A15) (see Refs. [35,36]), we then reach,

$$\begin{aligned}\dot{\rho}(t) = \alpha[&\sigma_-\rho(t)\sigma_+ - \rho(t)\sigma_+\sigma_-] + \beta[\sigma_+\rho(t)\sigma_-\\ &-\sigma_-\sigma_+\rho(t) - \sigma_-\rho(t)\sigma_+ + \rho(t)\sigma_+\sigma_-]\\ &+\alpha^*[\sigma_-\rho(t)\sigma_+ - \sigma_+\sigma_-\rho(t)] + \beta^*[\sigma_+\rho(t)\sigma_-\\ &-\rho(t)\sigma_-\sigma_+ - \sigma_-\rho(t)\sigma_+ + \sigma_+\sigma_-\rho(t)],\end{aligned} \tag{A18}$$

where α and β are given by

$$\alpha = \int_0^t d\tau \int_0^\infty d\omega\, g(\omega)|\kappa(\omega)|^2 e^{i(\omega-\omega_0)\tau}, \tag{A19}$$

and

$$\beta = \int_0^t d\tau \int_0^\infty d\omega\, g(\omega)|\kappa(\omega)|^2 e^{i(\omega-\omega_0)\tau}\bar{n}(\omega,\beta). \tag{A20}$$

Taking into account that the dynamics of the reservoir is much faster than the dynamics of the system, the limit of integration can be extended to infinity such that

$$\lim_{t\to\infty}\int_0^t d\tau\, e^{i(\omega-\omega_0)\tau} = \pi\delta(\omega-\omega_0) - i\frac{P}{\omega_0-\omega}, \tag{A21}$$

where P is the principal Cauchy value. In this way, we have

$$\alpha = \pi g(\omega_0)|\kappa(\omega_0)|^2 - i\Delta, \tag{A22}$$

and

$$\beta = \pi g(\omega_0)|\kappa(\omega_0)|^2\bar{n}(\omega_0,\beta) - i\Delta', \tag{A23}$$

with Δ and Δ' given by

$$\Delta = P\int_0^\infty d\omega \frac{g(\omega)|\kappa(\omega)|^2}{\omega_0-\omega}, \tag{A24}$$

and

$$\Delta' = P\int_0^\infty d\omega \frac{g(\omega)|\kappa(\omega)|^2\bar{n}(\omega_0,\beta)}{\omega_0-\omega}. \tag{A25}$$

Defining $\gamma = 2\pi g(\omega_0)|\kappa(\omega_0)|^2$ and neglecting the Lamb-shift term, one finally arrives at

$$\begin{aligned}\dot{\rho}(t) = &\frac{\gamma}{2}(1-n)[2\sigma_-\rho(t)\sigma_+ - \sigma_+\sigma_-\rho(t) - \rho(t)\sigma_+\sigma_-]\\ &\times\frac{\gamma}{2}n[2\sigma_+\rho(t)\sigma_- - \sigma_-\sigma_+\rho(t) - \rho(t)\sigma_-\sigma_+],\end{aligned} \tag{A26}$$

where $n \equiv \bar{n}(\omega_0,\beta)$. Eq. (1) is obtained by making the same deduction for three weakly interacting qubits, each one interacting with its respective thermal reservoir, and going back to the Schrödinger picture.

[1] J. Gemmer, M. Michel, and G. Mahler, *Quantum Thermodynamics: Emergence of Thermodynamic Behavior Within Composite Quantum Systems*, Lecture Notes in Physics (Springer, Berlin/Heidelberg, 2004).

[2] F. Binder, L. Correa, C. Gogolin, J. Anders, and G. Adesso, *Thermodynamics in the Quantum Regime: Fundamental Aspects and New Directions*, Fundamental Theories of Physics (Springer, Switzerland, 2019).

[3] P. Strasberg and A. Winter, PRX Quantum **2**, 030202 (2021).

[4] O. Abah, J. Roßnagel, G. Jacob, S. Deffner, F. Schmidt-Kaler, K. Singer, and E. Lutz, Phys. Rev. Lett. **109**, 203006 (2012).

[5] R. Alicki, Open Syst. Inf. Dyn. **21**, 1440002 (2014).

[6] A. Alecce, F. Galve, N. L. Gullo, L. Dell'Anna, F. Plastina, and R. Zambrini, New J. Phys. **17**, 075007 (2015).

[7] J. Roßnagel, S. T. Dawkins, K. N. Tolazzi, O. Abah, E. Lutz, F. Schmidt-Kaler, and K. Singer, Science **352**, 325 (2016).

[8] P. A. Camati, J. F. G. Santos, and R. M. Serra, Phys. Rev. A **99**, 062103 (2019).

[9] P. A. Erdman, V. Cavina, R. Fazio, F. Taddei, and V. Giovannetti, New J. Phys. **21**, 103049 (2019).

[10] J.-F. Chen, C.-P. Sun, and H. Dong, Phys. Rev. E **100**, 062140 (2019).

[11] M. J. Henrich, F. Rempp, and G. Mahler, Eur. Phys. J.: Spec. Top. **151**, 157 (2007).

[12] R. J. de Assis, J. S. Sales, J. A. R. da Cunha, and N. G. de Almeida, Phys. Rev. E **102**, 052131 (2020).

[13] U. C. Mendes, J. S. Sales, and N. G. de Almeida, J. Phys. B: At. Mol. Opt. Phys. **54**, 175504 (2021).
[14] A. El Makouri, A. Slaoui, and M. Daoud, J. Phys. B: At. Mol. Opt. Phys. (2023).
[15] L. D. Carr, Science **339**, 42 (2013).
[16] S. Braun, J. P. Ronzheimer, M. Schreiber, S. S. Hodgman, T. Rom, I. Bloch, and U. Schneider, Science **339**, 52 (2013).
[17] R. J. de Assis, C. J. Villas-Boas, and N. G. de Almeida, J. Phys. B: At. Mol. Opt. Phys. **52**, 065501 (2019).
[18] E. Abraham and O. Penrose, Phys. Rev. E **95**, 012125 (2017).
[19] H. Struchtrup, Phys. Rev. Lett. **120**, 250602 (2018).
[20] P. T. Landsberg, R. J. Tykodi, and A. M. Tremblay, J. Phys. A **13**, 1063 (1980).
[21] J.-Y. Xi and H.-T. Quan, Commun. Theor. Phys. **68**, 347 (2017).
[22] T. M. Mendonça, A. M. Souza, R. J. de Assis, N. G. de Almeida, R. S. Sarthour, I. S. Oliveira, and C. J. Villas-Boas, Phys. Rev. Res. **2**, 043419 (2020).
[23] E. Artacho and L. M. Falicov, Phys. Rev. B **47**, 1190 (1993).
[24] G. A. Álvarez, A. Ajoy, X. Peng, and D. Suter, Phys. Rev. A **82**, 042306 (2010).
[25] N. Linden, S. Popescu, and P. Skrzypczyk, Phys. Rev. Lett. **105**, 130401 (2010).
[26] P. Li and B. Jia, Phys. Rev. E **83**, 062104 (2011).
[27] A. Nüßeler, I. Dhand, S. F. Huelga, and M. B. Plenio, Phys. Rev. B **101**, 155134 (2020).
[28] L. Del Re, B. Rost, A. F. Kemper, and J. K. Freericks, Phys. Rev. B **102**, 125112 (2020).
[29] V. A. Mikhailov and N. V. Troshkin, Phys. Rev. A **103**, 012208 (2021).
[30] Emin Açıkkalp and N. Caner, Physica A **424**, 342 (2015).
[31] N. Van Horne, D. Yum, T. Dutta, P. Hänggi, J. Gong, D. Poletti, and M. Mukherjee, npj Quantum Inf. **6**, 37 (2020).
[32] K. Kaur, V. Singh, J. Ghai, S. Jena, and Ö. E. Müstecaplıoflu, Physica A **576**, 125892 (2021).
[33] G. Jiao, Y. Xiao, J. He, Y. Ma, and J. Wang, New J. Phys. **23**, 063075 (2021).
[34] G. G. Damas, R. J. de Assis, and N. G. de Almeida, arXiv:2204.09479.
[35] H. Breuer, P. Breuer, F. Petruccione, and S. Petruccione, *The Theory of Open Quantum Systems* (Oxford University Press, New York, 2002).
[36] A. Ghosh, S. S. Sinha, and D. S. Ray, Phys. Rev. E **86**, 011138 (2012).
[37] J. Johansson, P. Nation, and F. Nori, Comput. Phys. Commun. **183**, 1760 (2012).
[38] J. Johansson, P. Nation, and F. Nori, Comput. Phys. Commun. **184**, 1234 (2013).
[39] R. J. de Assis, T. M. de Mendonça, C. J. Villas-Boas, A. M. de Souza, R. S. Sarthour, I. S. Oliveira, and N. G. de Almeida, Phys. Rev. Lett. **122**, 240602 (2019).